ARTICLE INFO
Article ID: 2018-01-0820

doi:10.4271/2018-01-0820

Comparison of Active Front Wheel Steering and Differential Braking for Yaw/Roll Stability Enhancement of a Coach

Hongyu Zheng and Yangyang Miao, *Jilin University, China*
Bin Li, *Jilin University, China and Concordia University, Canada*

Abstract

Both active front wheel steering (AFS) and differential braking control (DBC) can improve the vehicle handling and stability. In this article, an AFS strategy and a DBC strategy are proposed and compared. The strategies are as follows: A yaw instability judging module and a rollover instability judging module are put forward to determine whether the coach is in a linear state and whether the additional torque/angle module should be actuated. The additional torque module based on linear quadratic regulator (LQR) and the additional steering wheel angle module based on adaptive proportion integral differential (PID) fuzzy controller are designed to make the actual yaw rate and sideslip angle track the reference yaw rate and sideslip angle. Under some typical driving conditions such as sinusoidal, J-turning, crosswind, and straight-line brake maneuver on the μ-split road, simulation tests are carried out for the coach with no control, DBC strategy, and AFS control, respectively. The comprehensive comparison of simulation results is made to verify the effectiveness of proposed strategies on improving vehicle handling and yaw stability. Results also show that the proposed two strategies can effectively prevent rollover of the vehicle and each has its own strengths for different maneuvers.

History

Received: 02 Dec 2017
Revised: 15 Apr 2018
Accepted: 16 Apr 2018
e-Available: 20 Dec 2018

Keywords

Active front wheel steering, Differential braking control, Yaw/roll stability control, LQR control, Adaptive PID fuzzy controller

Citation

Zheng, H., Miao, Y., and Li, B., "Comparison of Active Front Wheel Steering and Differential Braking for Yaw/Roll Stability Enhancement of a Coach," *SAE Int. J. Veh. Dyn., Stab., and NVH* 2(4):267-283, 2018, doi:10.4271/2018-01-0820.

ISSN: 2380-2162
e-ISSN: 2380-2170

WCX WORLD CONGRESS EXPERIENCE

This article is based on and revised or modified from a presentation at WCX18, Detroit, MI, April 10-12, 2018.

Introduction

With the progress of the society, travel modes are various. As a convenient and fast means of transportation, coaches have a great prospect. Coaches run under various road conditions. The mass center of coaches is high and easily affected by passengers. Under extreme conditions, coaches are prone to be unstable. The reaction time and unfamiliarity with road conditions of the driver also make the control of coach more difficult. Once the coach becomes unstable and rollover occurs, it will not only cause many injuries and deaths but also cause a serial accident on the highway due to the delay of the surviving passenger evacuation. Therefore, it is of great significance to study the active safety technology for the coaches [1].

Differential braking technology is used to calculate the best extra yaw moment. To find the best braking torque, there are many methods put forward to control the handling stability of the vehicle, including proportion integral differential (PID) control, optimal control, fuzzy control, Lyapunov stability control, nonlinear H-infinity control, sliding mode control, rollover threshold control, etc. [2, 3]. Chen et al. proposed a time-to-rollover (TTR) algorithm to prevent rollover of the vehicle and concluded that the TTR can effectively prevent the rollover [4]. Esmailzadeh et al. presented two optimal yaw moment controllers, the semi-optimal controller and the optimal controller, based on the optimal control theory. The simulation results showed that the semi-optimal controller is more appropriate than the optimal controller [5]. Fujimoto et al. proposed a road condition estimation and anti-slip controller to stabilize the vehicle by an inner-loop observer and an outer-loop controller [6]. Kyongsu et al. proposed a sliding controller as brake control input to control the stability of vehicles [7]. Mizushima et al. proposed two types of desired yaw rate, lane keeping control and vehicle stability control, by using the application of hidden Markov model (HMM) and adopted the theory of probability to recognize the two types [8]. Zhang et al. presented a vehicle yaw stability control strategy integrated with active torque distribution and differential braking system [9]. Ghosh et al. put forward a yaw stability system based on fuzzy controller. The controller was consistent with sensorimotor in humans and effectively supported the steering assistance system [10]. Brad et al. proposed a yaw stability controller based on Lyapunov stability and a rollover control strategy based on a rollover threshold [11]. Tchamna et al. proposed a sliding mode controller applied to differential braking [12]. Elhefnawy et al. presented an active roll control and a direct yaw control system to improve both the rollover and cornering stability of the vehicle [13]. Yu et al. proposed a rollover warning (RW) system and adopted a fuzzy controller to produce additional yaw moment from differential braking [14].

For active steering, the optimal additional angle needs to be calculated. Many control methods [15, 16, 17, 18, 19, 20, 21, 22] are proposed to calculate the additional steering angle, including optimal control theory, sliding mode control, particle swarm optimization algorithm, etc. In these studies, most of research is aimed at cars. Klier et al. elaborated the respective advantages and requirements of modular system concept of AFS on BMW 5-series [15]. Oraby et al. proposed an active steering control strategy based on the optimal control theory and compared the active front-steering control with active four-wheel steering and conventional two-wheel steering [16]. Walid et al. proposed an optimal AFS model based on the optimal control theory using linear quadratic regulator (LQR) and compared the optimal AFS with the conventional two-wheel steering in the process of overtaking [17]. Zheng et al. presented an AFS strategy based on the feedback of both yaw rate and front-steering angle [18]. Truong et al. presented a dynamic sliding mode controller based on Lyapunov theory to improve vehicle handling maneuver and path tracking performance of sport utility vehicles [19]. Elmi et al. proposed an active front-steering controller based on a LQR controller [20]. Xu et al. studied the kinematics and dynamics of AFS and proposed a basic control on a DC motor [21].

In the above references, AFS and DBC can only work well in the specific handling region. The maximum benefit could be gained by AFS and DBC integrated control strategies [22, 23, 24, 25, 26]. Coaches have hysteresis characteristic with pneumatic braking. Compared with cars, the steering response of coaches is relatively slow with a large front axle load. The high centroid and the large passenger capacity make it more important in security. How to better improve the safety of coach is of great significance. However, there are few previous studies on steering and braking of coaches. Besides, there is no mature active safety system integrating AFS and DBC in the market. It is the case that the steering and braking are controlled separately for a long time. Therefore, a control strategy based on DBC and a control strategy based on AFS are put forward in this article.

In this article, an AFS control strategy based on a fuzzy PID self-tuning controller and a DBC strategy based on a LQR controller are proposed. The yaw instability judgment module and RW module are adopted in the DBC and AFS to judge whether the coach is in a stable state. Sinusoidal, J-turn, straight-line brake on the μ-split road, and crosswind operation maneuvers are simulated to compare the different responses of the two strategies on the coach. Simulation shows that both DBC and AFS can prevent yaw and rollover instability through active intervention under various extreme conditions. AFS and the DBC can enhance the handling stability and effectively prevent rollover of the coach, but each has its own strengths.

The difference between AFS and DBC of the coach is compared in this article, which includes three parts: yaw stability control strategy, rollover stability control strategy, and the conclusion. The following sections—the two degrees of freedom (DOF) reference vehicle model, the instability judgment module, the additional torque/angle module, the adaptive PID fuzzy controller, and the brake force distribution module-are employed in the two strategies. Therefore, three controllers, LQR controller, fuzzy controller, and fuzzy PID self-tuning controller, are employed in the DBC and AFS to calculate the additional moment/steering wheel angle.

The sinusoidal maneuver is used to compare the responses of the three controllers. Then the J-turn maneuver, straight-line brake maneuver on the μ-split road, and straight-line driving maneuver under the crosswind are simulated to compare the different responses of the DBC and AFS. The second part, rollover stability control strategy, the DBC and AFS are also employed, which includes the 3-DOF reference model, the RW module, and the additional torque calculation module. Then the sinusoidal maneuver and J-turn maneuver are conducted to compare the DBC and AFS.

Yaw Stability Strategy of a Coach

Under the influence of vertical load and steering mechanism, tires in contact with the ground will produce side deflection and lateral forces. The lateral forces provide the centripetal force required for the steering. There will be a yaw motion when the vehicle is cornering. And the lateral forces at the front and rear wheels will produce an additional yaw moment to the vehicle centroid. Therefore, the actual vehicle motion may deviate from the driver's intention.

When the vehicle is cornering or braking on the μ-split road, the longitudinal forces at the left and right wheels are unequal, resulting in additional yaw moment of the vehicle which will cause yaw instability of the vehicle. Tires cornering characteristics mainly refer to the relationship between the lateral force, self-aligning torque, and the tire slip angle. Assume that side deflection property of the tire is not considered. When the vehicle turns at low speed, the required centripetal force of the vehicle is small, and the deformation of the tire and suspension spring can be neglected. When the vehicle is turning at high speed, tires produce greater lateral forces to provide the required centrifugal force. The different slip angles of front and rear wheels will influence actual turning radius.

Differential Braking Control Strategies

When the vehicle makes a sharp turn, the slip angles of the tires increase sharply. The lateral forces reach limit values quickly and cannot meet the demand during cornering. If lateral forces at the front wheels reach saturation first and do not provide enough centripetal force, it will cause understeer; if lateral forces at the rear wheels reach saturation first, it will cause oversteer. At this time if a brake is applied to the individual wheel of the vehicle, the braking force will produce an additional yaw moment, which will change the original yaw moment, and then the vehicle state is changed. Besides, the braking force not only reduces longitudinal force but also changes the lateral force limit value of tires. The method of controlling individual wheel braking is called differential braking, which improves the vehicle yaw stability and maneuverability.

In the DBC strategy for yaw stability of the coach, three additional torque calculation methods are proposed and compared. Yaw stability control strategy of the DBC is as follows: TruckSim software delivers the longitudinal speed and the front wheel angle to the 2-DOF vehicle model. And the 2-DOF model outputs the reference yaw rate and the sideslip angle. The reference yaw rate and sideslip angle and the actual values from TruckSim are delivered to the instability judgment module to determine whether additional yaw moment is needed. If the module output is true, it will trigger the additional torque calculation module to calculate the optimal additional yaw moment. Then the braking force distribution module determines which wheel to brake and turns the additional yaw moment into brake force and then brakes the corresponding wheel in TruckSim software. The Appendix at the end of the article presents the main parameters of the coach.

Active Front Wheel Steering Control Strategies

In the design of the vehicle steering system, the steering handiness and the steering sensitivity are contradictory. Portability means the driver exerts less force on the steering wheel. Sensitivity means the driver turns the steering wheel to the target angle quickly. It is a contradiction that the transmission ratio should be reduced for a high sensitivity as well as increased for a high portability. The AFS has variable transmission ratio, which can solve the contradiction of steering handiness and agility. The AFS system can apply a steering intervention independent of the driver, which can change the transmission ratio within a certain range and improve the handling stability at the same time.

In the AFS control strategy for yaw stability of the vehicle, three additional steering wheel angle calculation methods are compared to calculate optimal additional steering wheel angle. The 2-DOF model outputs reference yaw rate and sideslip angle, which are compared with the real values output by TruckSim software. If the result is beyond the linear regime of the coach, the additional angle module will be actuated to increase or decrease the additional steering wheel angle.

2-DOF Reference Vehicle Model Coach is a complex body with multiple DOF. In the yaw stability analysis, the ideal yaw rate and sideslip angle are required. The more DOF of the coach model, the closer to the real coach, the more actual the yaw rate and sideslip angle are. Therefore, the ideal yaw rate and sideslip angle can be obtained by simplifying the vehicle model to yaw motion and lateral motion. Thus, only the longitudinal speed and the front wheel angle of the coach are needed. Other directions such as vertical and roll motions should be ignored. The coach is reduced to a 2-DOF model (as shown in Figure 1) which only considers the yaw motion and lateral movement of the coach. 2-DOF model is widely used as reference vehicle model [19].

FIGURE 1 Simplified 2-DOF model.

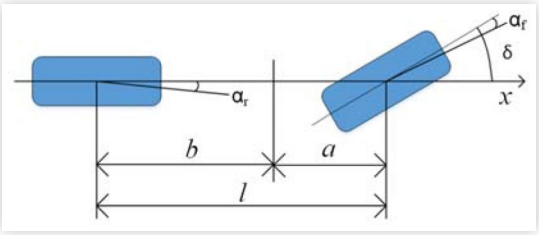

The dynamic differential equations are given as below:

$$\dot{\omega}_r = \frac{a^2k_1 + b^2k_2}{I_Z v_x}\omega_r + \frac{ak_1 - bk_2}{I_Z}\beta - \frac{ak_1}{I_Z}\delta_f \qquad \text{Eq. (1)}$$

$$\dot{\beta} = \left(\frac{ak_1 - bk_2}{mv_x^2} - 1\right)\omega_r + \frac{k_1 + k_2}{mv_x}\beta - \frac{k_1}{mv_x}\delta_f \qquad \text{Eq. (2)}$$

The yaw rate steady-state gain $G_f(s)$ of the coach can be obtained from the state equation above:

$$G_f(s) = \frac{\omega_r(s)}{\delta_f(s)} \approx \frac{K_a}{\tau s + 1} \qquad \text{Eq. (3)}$$

$$K_a = \frac{v_x}{l + \frac{m}{l}\left(\frac{b}{k_1} - \frac{a}{k_2}\right)v_x^2} = \frac{v_x / l}{1 + \frac{m}{l^2}\left(\frac{a}{k_2} - \frac{b}{k_1}\right)v_x^{\,2}} = \frac{v_x}{l\left(1 + K_{us}v_x^2\right)} \qquad \text{Eq. (4)}$$

$$\tau = \frac{v_x a k_1}{I_z\left[l + \frac{m}{l}\left(\frac{b}{k_1} - \frac{a}{k_2}\right)v_x^2\right]} \qquad \text{Eq. (5)}$$

where τ is the delay time constant and K_{us} is the stability factor.

When $K_{us} > 0$, the actual turning radius is larger than the predetermined turning radius, and the coach is understeer. When $K_{us} < 0$, the actual turning radius is less than the predetermined turning radius, and the coach is oversteer. When $K_{us} = 0$, the coach has a neutral steering, and the actual turning radius is equal to the predetermined turning radius.

The total transmission ratio of the steering system is i:

$$i = \frac{\delta_{sw}}{\delta_f} \qquad \text{Eq. (6)}$$

where δ_{sw} is the steering wheel angle and δ_f is the front wheel angle.

Equations 3 and 6 are combined and the transmission ratio is expressed as:

$$i = \frac{K\delta_{sw}}{(\tau s + 1)\omega_r} = \frac{K}{(\tau s + 1)G} \qquad \text{Eq. (7)}$$

$$G = \frac{\omega_r}{\delta_{sw}} \qquad \text{Eq. (8)}$$

The vehicle system gain G is the ratio of the yaw rate to the steering wheel angle. Steering system gain G_s is the ratio of the front wheel angle to the steering wheel angle. The relationship is $G = G_sG_f$. If the yaw rate steady-state gain G_f remains constant, the steering system gain G_s varies with the coach speed, and the vehicle system gain G varies with the vehicle speed:

$$G_s = \frac{\delta_f}{\delta_{sw}} \qquad \text{Eq. (9)}$$

$$i = \frac{G_f}{(\tau s + 1)G} \qquad \text{Eq. (10)}$$

The stability factor and the longitudinal speed play an important role in yaw stability of the vehicle. The stability factor at high speeds should ensure the stability of the vehicle. Therefore, the actual turning radius of the vehicle had better be equal to or slightly greater than the desired turning radius. Therefore, a neutral steering or a slight understeer is the ideal state of the vehicle during cornering.

Instability Judgment Module When the vehicle takes a sharp turn or is affected by crosswind, the lateral forces may close to the adhesion limit or reach saturation. The vehicle will quickly lose dynamic stability especially coaches with high centroid. At this time, the cornering characteristics of tires have entered the nonlinear region. Since yaw rate and sideslip angle can appropriately describe vehicle dynamic stability, the stability of coach can be determined by the difference between the actual values and the ideal values. When the difference is small, the vehicle is in a stable state; when the difference exceeds the predetermined range, the control system should take the initiative to stabilize the coach. The relationship of sideslip angle and sideslip rate can be satisfied as Equation 11 which is obtained from the experiment of [27]. The reference yaw rate and actual yaw rate need to satisfy Equation 12. When Equations 11 and 12 are tenable, the coach has a good handling stability. If not, the coach will be in an unstable state.

Taking step steering input at different speeds as an example, with 180 degree angle of steering wheel, the sideslip angle and sideslip rate phase diagram are obtained as shown in Figure 2. The transverse coordinate is sideslip angle, and the longitudinal coordinate is sideslip rate. Figure 2 shows that the region between the two red lines reveals the coach is stable and the area out of the two red lines reveals the coach is unstable, which means active control are needed. The stable region within the two red lines is consistent with Equations 11 and 12.

$$\left|C_1\beta + C_2\dot{\beta}\right| \le 1 \qquad \text{Eq. (11)}$$

$$\left|\omega_r - \omega_{r0}\right| < \left|C\omega_{r0}\right| \qquad \text{Eq. (12)}$$

where ω_r is the actual yaw rate, ω_{r0} is the reference yaw rate, and C is a constant.

Additional Torque/Angle Calculation Module The optimal control system has the maximum or minimum value index of the system under the required constraints. LQR is employed to calculate the optimal additional yaw moment

FIGURE 2 The phase diagram of sideslip angle and sideslip rate.

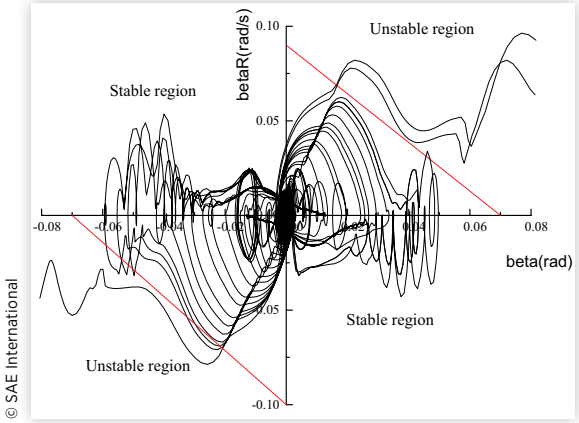

required to stabilize the coach. The purpose is to make the yaw rate and sideslip angle approach the reference values as far as possible. The linear continuous state equation of the coach is:

$$\dot{x}(t) = Ax(t) + Bu(t) \qquad \text{Eq. (13)}$$

The optimal control index can be expressed as follows:

$$J = \int_0^\infty \left[x(t)^T Qx(t) + u(t)^T Ru(t) \right] dt \qquad \text{Eq. (14)}$$

Matrices Q and R are the symmetric positive definite weighting matrix. Search for appropriate Q and R to get the best index. Under the premise of given system (13) and confined index (14), a controller u is designed to minimize J. The optimal controller u can be written as follows:

$$u = -R^{-1}B^T Px = -Kx \qquad \text{Eq. (15)}$$

Equation 15 is substituted into Equation 13:

$$\dot{x} = (A - BK)x \qquad \text{Eq. (16)}$$

There must be a positive definite symmetric matrix P of quadratic *Lyapunov* function $V(x) = x^T Px$ based on the *Lyapunov* stability theorem of linear time-invariant systems. The matrix P is used into Equation 17 and the result is:

$$\begin{aligned} J &= \int_0^\infty \left[x^T Qx + u^T Ru + \frac{d}{dt} V(x) \right] dt - \int_0^\infty \frac{d}{dt} V(x) \cdot dt \\ &= \int_0^\infty \left\{ x^T Qx + u^T Ru + x^T \left[P(A - BK) + (A - BK)^T P \right] x \right\} dt \\ &\quad - V\left[x(t) \right] \Big|_{t=0}^{t=\infty} \\ &= \int_0^\infty x^T \left[Q + \underline{K^T RK} + PA + A^T P \underline{- PBK} \underline{- K^T B^T P} \right] x dt + x_0^T Px_0 \end{aligned} \qquad \text{Eq. (17)}$$

The squares of the underlined parts of the equation above can be obtained as follows:

$$\begin{aligned} &\underline{K^T RK} \underline{- PBK} \underline{- K^T B^T P} + PBR^{-1}B^T P - PBR^{-1}B^T P \\ &= \left(K - R^{-1}B^T P \right)^T R \left(K - R^{-1}B^T P \right) - PBR^{-1}B^T P \end{aligned} \qquad \text{Eq. (18)}$$

The formula above is rewrote and the result is:

$$\begin{aligned} J &= \int_0^\infty x^T \left[Q + PA + A^T P - PBR^{-1}B^T P \right] x dt + x_0^T Px_0 \\ &\quad + \int_0^\infty x^T \left(K - R^{-1}B^T P \right)^T R \left(K - R^{-1}B^T P \right) x dt \end{aligned} \qquad \text{Eq. (19)}$$

Only if the third item equals zero that the performance index J obtained by Equation 19 can be minimum. Only if the matrix K satisfies the following relationship that the third item equals zero:

$$K = R^{-1}B^T P \qquad \text{Eq. (20)}$$

The matrix K relies on the positive definite symmetric matrix P and meets the *Riccati* equation:

$$PA + A^T P - PBR^{-1}B^T P + Q = 0 \qquad \text{Eq. (21)}$$

Closed-loop system equation is as follows:

$$\dot{x} = \left(A - BR^{-1}B^T P \right) x \qquad \text{Eq. (22)}$$

The optimal state feedback controller u is:

$$u = -R^{-1}B^T P_x \qquad \text{Eq. (23)}$$

The state Equation 13 is adopted in the controller design. In the additional torque calculation, the state variable is $x(t) = [\Delta\beta\ \Delta\omega_r]^T$, and the control variable is $u = \Delta M_z$. And the matrices A and B are as follows:

$$A = \begin{bmatrix} \dfrac{k_1 + k_2}{mv_x} & \dfrac{ak_1 - bk_2}{mv_x^2} - 1 \\ \dfrac{ak_1 - bk_2}{I_Z} & \dfrac{a^2 k_1 + b^2 k_2}{I_Z v_x} \end{bmatrix}, \quad B = \begin{bmatrix} 0 \\ -\dfrac{\Delta M_z}{I_z} \end{bmatrix} \qquad \text{Eq. (24)}$$

In the additional steering wheel calculation, the state variable is $x(t) = [\Delta\beta\ \Delta\omega_r]^T$, and the control variable is $u = \delta_{af}$. And the matrices A and B are as follows:

$$A = \begin{bmatrix} \dfrac{k_1 + k_2}{mv_x} & \dfrac{ak_1 - bk_2}{mv_x^2} - 1 \\ \dfrac{ak_1 - bk_2}{I_Z} & \dfrac{a^2 k_1 + b^2 k_2}{I_Z v_x} \end{bmatrix}, \quad B = \begin{bmatrix} -\dfrac{k_1}{mv_x} \\ \dfrac{ak_1}{I_Z} \end{bmatrix} \qquad \text{Eq. (25)}$$

Adaptive PID Fuzzy Controller Fuzzy control is a mathematical model which does not need precise mathematical relation and has no dependence on controlled object. Therefore, it is easy to implement.

The input and output variables of the fuzzy controller are selected as follows:

{Negative Big, Negative Medium, Negative Small, Zero, Positive Small, Positive Medium, Positive Big}

Abbreviations are as follows:

{*NB*, *NM*, *NS*, *ZE*, *PS*, *PM*, *PB*}

The fuzzy control in this study adopts the gravity defuzzification method. The final output value is the gravity center

of the area formed by the fuzzy membership function curve and abscissa. The output is as follows:

$$v_0 = \frac{\int_V v u_v(v) dv}{\int_V u_v(v) dv} \quad \text{Eq. (26)}$$

For discrete fields with m outputs quantization series, the output is as follows:

$$v_0 = \frac{\sum_{k=1}^{m} v_k u_v(v_k)}{\sum_{k=1}^{m} u_v(v_k)} \quad \text{Eq. (27)}$$

The yaw rate error is the input of the fuzzy controller. The fuzzy control rule is that when the yaw rate error reaches the negative maximum value, fuzzy controller makes the yaw torque the positive maximum. When the yaw rate error reaches positive maximum value, fuzzy controller will make the yaw torque negative maximum.

The PID control law is as follows:

$$u(t) = K_p e(t) + K_I \int_0^t e(t) dt + K_D \frac{de(t)}{dt} \quad \text{Eq. (28)}$$

where K_P is the proportionality coefficient, K_I is the integral coefficient, and K_d is the differential coefficient.

The function of K_P is to speed up the response of the system. If K_P is too large, it will produce overshoot and oscillation; if K_P is too small, it will reduce adjustment accuracy, slow down system response speed, prolong adjustment time, and increase steady-state error. The function of K_I is to eliminate the steady-state error of the system. If K_I is too small, the integral function becomes weak, and the static error is difficult to eliminate. The role of K_d is to improve the dynamic performance of the system. To make these three parameters meet self-tuning requirements at a different time, the fuzzy controller outputs parameters K_P, K_I, K_d modification real time online.

Brake Force Distribution Module In this article, single wheel brake is used at first. When the braked wheel is locked, another wheel on the same side will be used. Taking the rear outer wheel brake as an example, during the turning process, when the rear outer wheel is braked, the additional ground force generated by braking will provide outward additional yaw moment to the center of mass. The required additional yaw moment can be designed as:

$$\Delta M = -\left(F_x' - F_x\right)\frac{T}{2} - \left(F_y' - F_y\right)b \quad \text{Eq. (29)}$$

where ΔM is the additional yaw moment produced by rear outer brake, F_x is the longitudinal force when there is no brake, F_x' is the longitudinal force when brake is acted, F_y is the lateral force when there is no brake, F_y' is the lateral force when brake is acted, T is the wheel track, and b is the distance between gravity center and rear axle. With the increase of braking force, longitudinal force provided by the ground gradually increases to the boundary of the attached ellipse. The lateral force F_y' begins to decrease along the attached ellipse boundary, and the longitudinal force increases slowly.

FIGURE 3 Influence of single braking force for yaw moment absolute value.

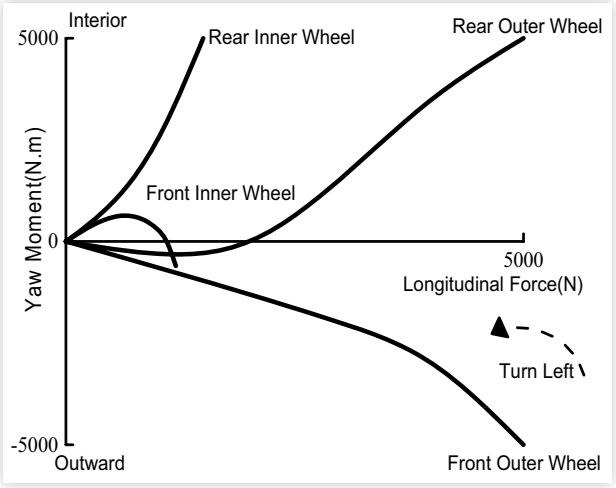

The outward yaw moment provided by the original rear outer wheel ground force will decrease and gradually become inward yaw moment. When the brake is increasing constantly, the wheel will get locked and slipped and then the lateral force will reduce to zero. The longitudinal force F_y' will no longer change without considering speed change, and the additional yaw moment is positive and constant. Or the longitudinal force F_y' will decrease considering speed reduction and the additional yaw moment is positive and becomes lager. When F_y is zero, ΔM is $\Delta M = F_x \frac{T}{2} + F_y b - F_x' \frac{T}{2}$.

The relationship of braking force and yaw moment absolute value on the coach is shown in Figure 3 when braking force is applied to the individual wheel. Braking the rear inner wheel can increase the yaw moment absolute value of the coach and reduce understeer when cornering. Braking the front outer wheel can reduce the yaw moment absolute value and reduce oversteer during cornering. Braking the front inner wheel can increase the yaw moment absolute value and reduce the understeer in the beginning when cornering. But the yaw moment will decrease to negative value in the next time, and the zero point is uncontrollable. Similarly, braking the rear outer wheel can reduce the yaw moment absolute value and reduce oversteer in the beginning. But the yaw moment will increase to positive value in the next time, and the zero point is uncontrollable.

Assume that the left turn is positive. The front wheel angle and the difference of the yaw rate determine the steering type and the brake wheel. Table 1 shows the braking force distribution of the coach.

TABLE 1 Brake force distribution.

Front wheel angle	Yaw rate difference	Steering type	Braking wheel
$\delta_f > 0$	$\Delta\omega_r > 0$	Oversteer	Right wheels
$\delta_f > 0$	$\Delta\omega_r < 0$	Understeer	Left wheels
$\delta_f < 0$	$\Delta\omega_r > 0$	Understeer	Right wheels
$\delta_f < 0$	$\Delta\omega_r < 0$	Oversteer	Left wheels

The ground braking force at the left wheels can be obtained as follows:

$$F_{xfl} = \frac{2\Delta M}{T\cos\delta_f}$$
$$F_{xrl} = \frac{2\Delta M}{T} \quad \text{Eq. (30)}$$

where F_{xfl} is the longitudinal force on the left front wheel and F_{xrl} is the longitudinal force on the left rear wheel.

The calculation of the ground braking force at the right wheels is similar.

Simulation Results

TruckSim is a simulation software specially designed for vehicle dynamics, which provides various types of vehicle model database including medium to heavy trucks, buses, trailers, and so on. Compared with the multi-degree of freedom of vehicle model based on the actual vehicle test parameters, the vehicle model in TruckSim is more consistent with the actual vehicle and it also avoids the impact when the parameters are equivocal. Therefore, TruckSim is used as the actual vehicle model for simulation in this article.

Sinusoidal Maneuver The sinusoidal maneuver, as shown in Figure 4, is that the steering wheel turns 180 degrees to the left and returns to the origin within 2.5 seconds, and then the steering wheel rotates 180 degrees to the right and returns to the origin in the next 2.5 seconds.

The road adhesion coefficient is 0.85. Under uncontrolled circumstances, as shown in Figure 5, the coach can go back to steady state at 65 km/h after a sinusoidal maneuver. When the coach is running at the speed of 66 km/h, the yaw rate is close to the curve of 65 km/h, but the coach cannot return to steady state and rollover occurs. So, 66 km/h is the critical speed of the coach in the sinusoidal maneuver. The coach turned over in 4.5 seconds at the speed of 70 km/h. Therefore, 70 km/h is selected to validate the proposed strategies.

FIGURE 4 Steering wheel angle under sinusoidal maneuver.

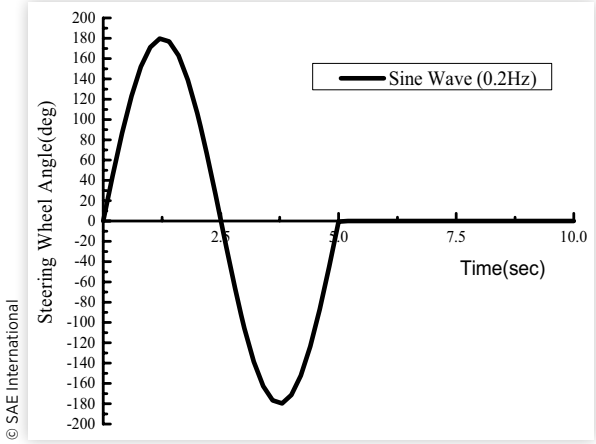

FIGURE 5 Vehicle response under sinusoidal maneuver.

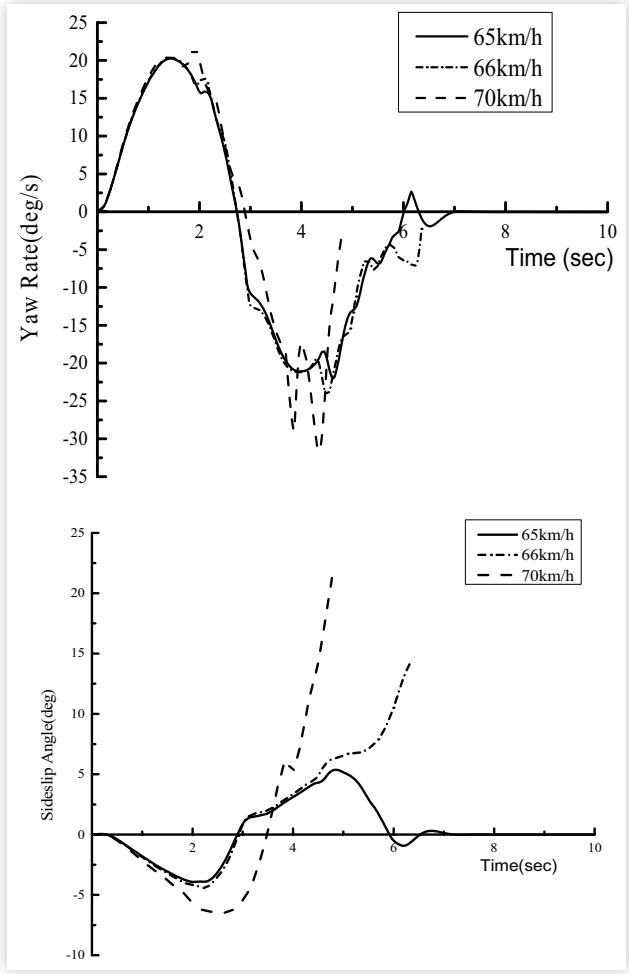

In the DBC strategy, the effectiveness of three control methods presented previously is compared in the sinusoidal maneuver. As shown in Figure 6, LQR controller has the best performance; fuzzy PID self-tuning controller is better than fuzzy controller but inferior to LQR controller. LQR controller has a good control effect on the yaw rate, sideslip angle, and roll angle. Therefore, LQR controller is adopted in the DBC strategy in the later introduction.

In the AFS control, the results with three control methods proposed previously are also compared. As shown in Figure 7, fuzzy PID self-tuning controller shows the best performance; fuzzy controller and LQR controller are inferior to it. Adaptive PID fuzzy controller has a good control performance on the stability of the coach. Therefore, fuzzy PID self-tuning controller is adopted in the AFS strategy in the later sections.

It can be concluded that both AFS and DBC can enhance the stability and mobility of the coach. As shown in Figure 8, the pros and cons of the two methods are compared as follows, and it is concluded that the DBC has a better performance and can make the vehicle states better follow the reference curves than AFS in the sinusoidal maneuver. The above sinusoidal experiment is simulated on the road adhesion

FIGURE 6 Vehicle response with DBC strategy under sinusoidal maneuver.

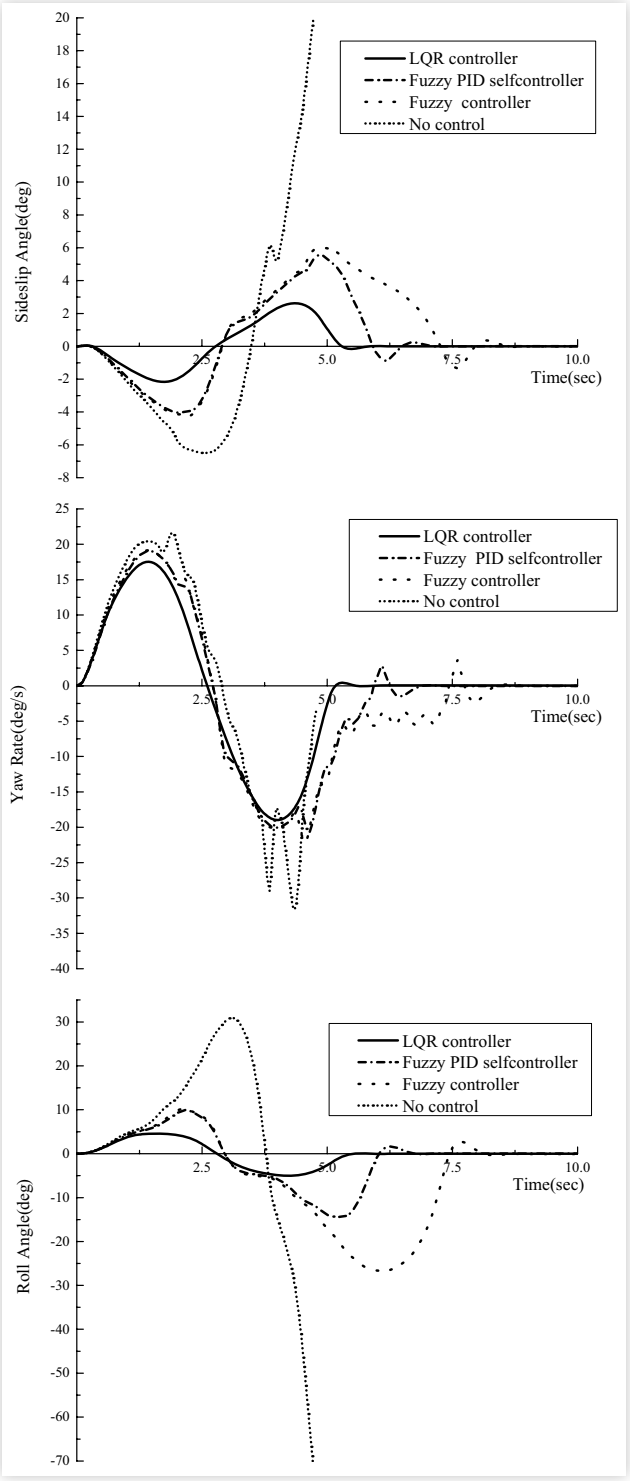

FIGURE 7 Vehicle response with AFS control under sinusoidal maneuver.

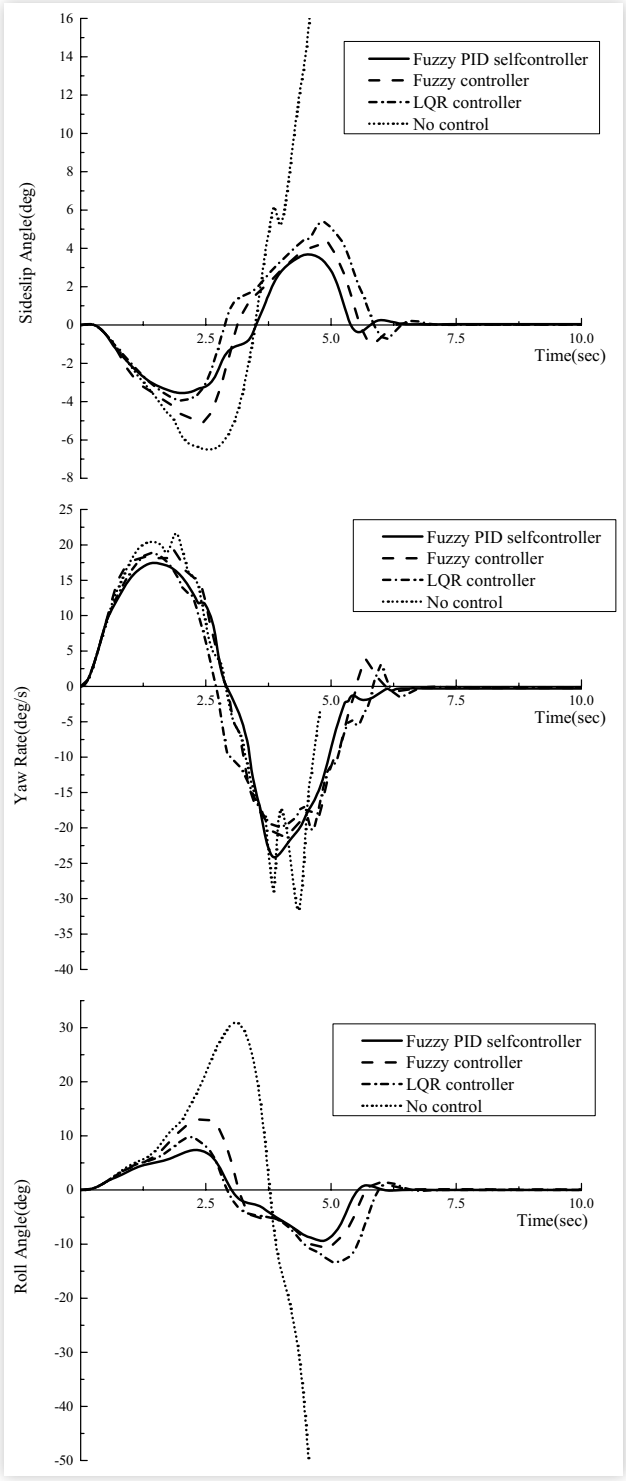

FIGURE 8 Comparison of vehicle response with AFS and DBC under sinusoidal maneuver.

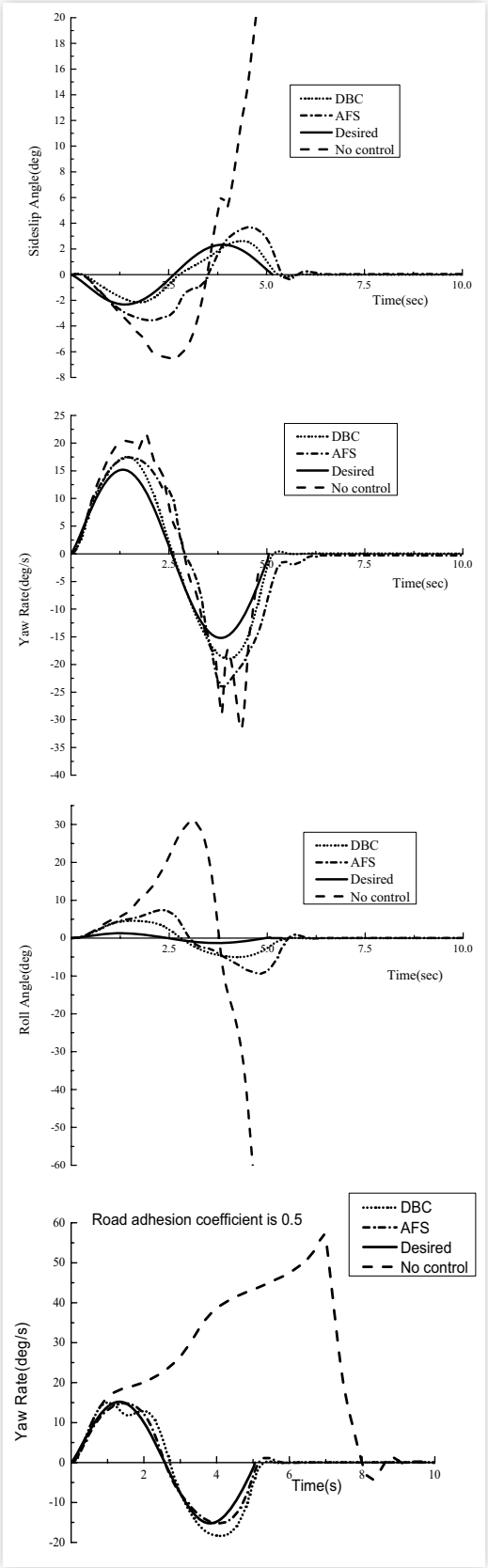

FIGURE 9 Steering wheel angle under J-turn maneuver.

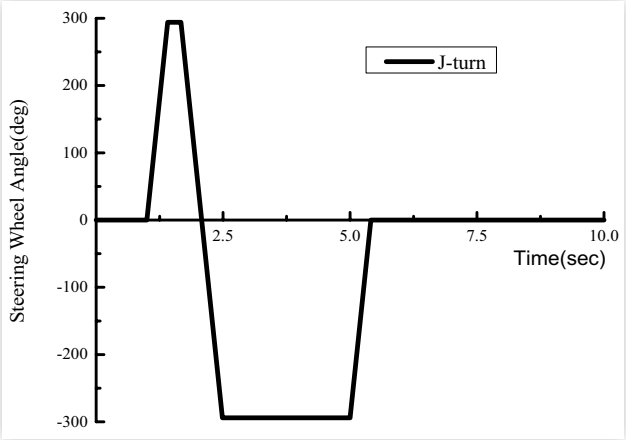

coefficient 0.85. When the road adhesion coefficient is reduced to 0.5, the lateral force is insufficient, and the coach under no control does not rollover. It loses its direction and leads to a large overturn. As shown in the figure, AFS can better track the desired values than DBC when the road adhesion is low.

J-Turn Maneuver J-turn, as shown in Figure 9, is that the steering wheel rapidly rotates 298 degrees to the left within 0.4 seconds, holds 0.2 seconds, then rapidly rotates 596 degrees to the right within 0.8 seconds, holds 2.5 seconds, and then turns back to the origin within 0.4 seconds.

Under no control strategy, as shown in Figure 10, the coach can go back to steady state at the speed of 43 km/h after the J-turn maneuver. It can be found that the curve of 44 km/h is close to the curve of 43 km/h in the beginning, but it had a rollover in 5 seconds and cannot return to the steady state. So, 44 km/h is considered as the critical speed of the coach in the J-turn maneuver. The coach turns over in 4 seconds at 45 km/h.

AFS and DBC strategies are validated with open-loop steering at 80 km/h. The steering wheel input of the driver is zero. The simulation shows that the coach under no control is going to roll at the time of 2.5 seconds in the J-turn maneuver. Comparing the two strategies, as shown in Figure 11, it can be concluded that the AFS has a better handling performance than the DBC in J-turn maneuver, while DBC has a better path tracking ability.

Straight-Line Brake Maneuver on the μ-Split Road In winter, because of the ice and snow on the road, the road adhesion coefficient between the left and right wheels of coaches is usually different. In this article, left road adhesion coefficient of the μ-split road is set to 0.2 and the right is 0.5. The coach runs at 120 km/h on the μ-split road; the control effect of the two strategies is shown in Figure 12.

The slip ratio for each wheel is given as below:

$$s = 1 - \frac{r \cdot \omega}{v_x} = 1 - \frac{v_i}{v_x} \qquad \text{Eq. (31)}$$

where r is wheel rolling radius, ω is wheel angular velocity, and v_i is the speed of each wheel.

FIGURE 10 Sideslip angle and yaw rate response under J-turn maneuver.

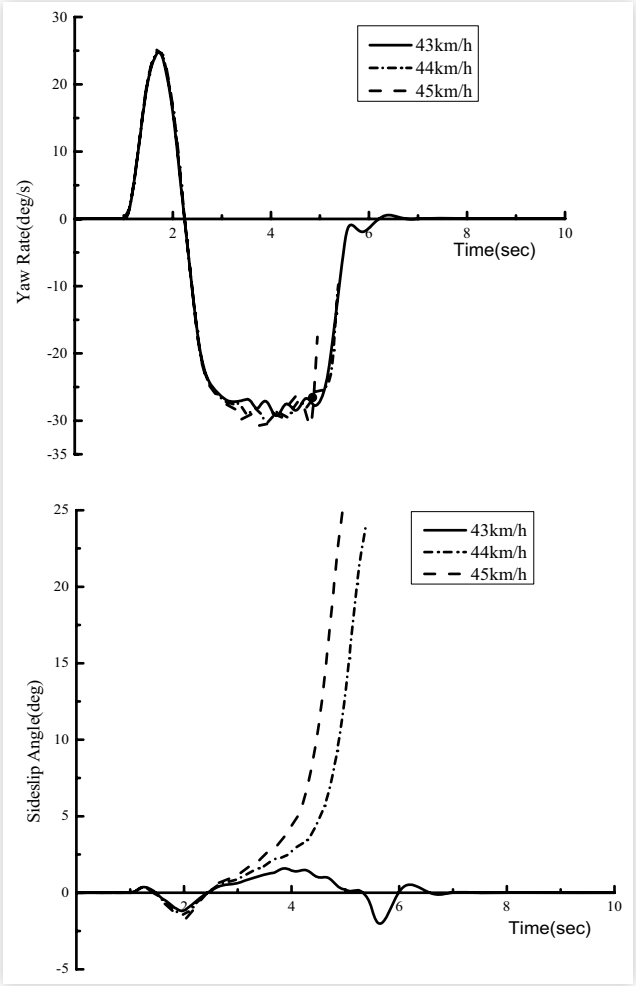

FIGURE 11 Comparison of vehicle response with AFS and DBC under J-turn maneuver.

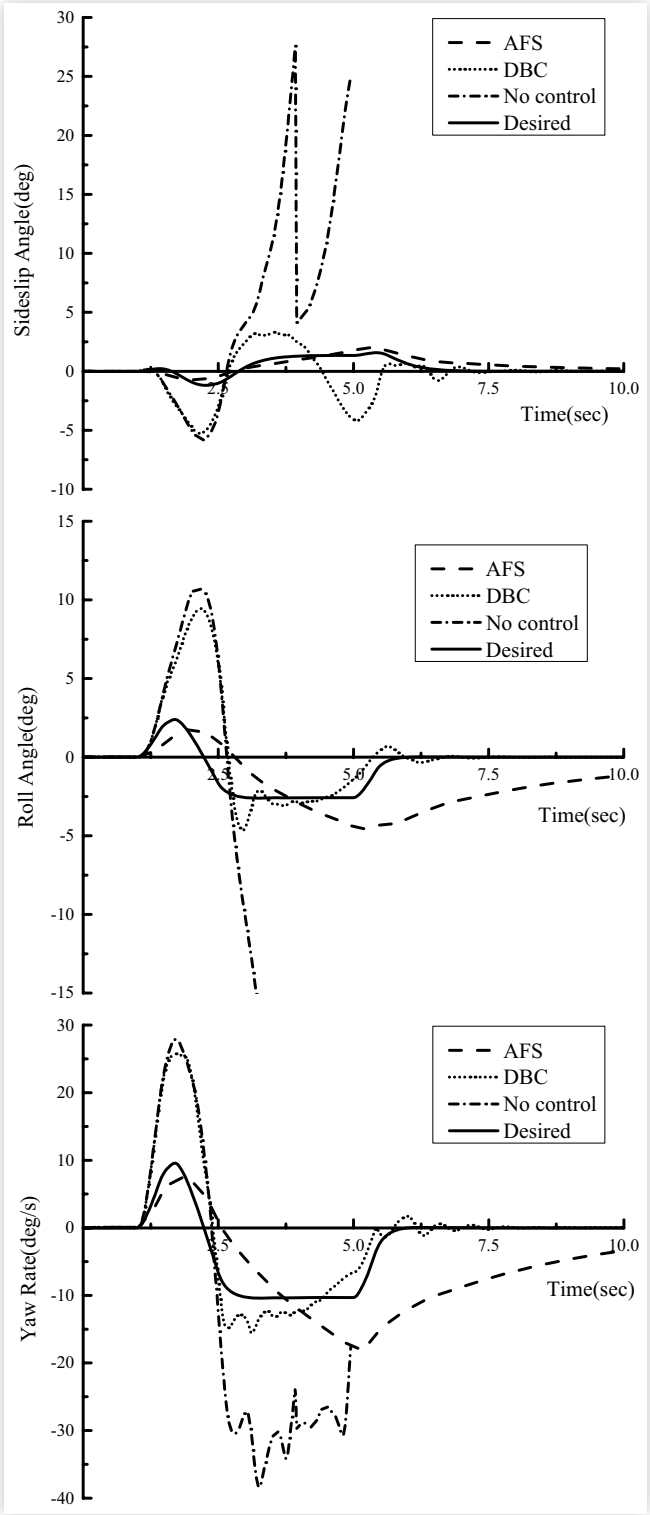

The slip ratio should be controlled between 0.05 and 0.15. The lower slip ratio of the rear wheels is selected as the control objective. When the slip ratio between the rear wheels and the front wheels exceeds the set value, the brake holds the pressure until the slip ratio of the rear wheels is reduced to the setting ratio. Anti-lock brake system (ABS) is applied in the operation and is compared with the AFS and DBC.

As shown in Figure 12, the simulation shows that the coach under no control rotates 360 degrees from the 6th second to the 16th second. ABS control shows the shortest brake distance and the best performance in the braking on the opposite and split road. DBC method has a shorter brake distance than the AFS but longer than ABS control. DBC and AFS have similar control effect in yaw rate and sideslip angle. The rear outer wheel speed plots are shown in Figure 13. ABS, DBC, and AFS all can prevent rear outer wheel lockup. ABS control directly takes the slip ratio of the wheel as the control objective, and it can brake steadily with very small fluctuations. The speed fluctuation of DBC is slightly larger than ABS during the braking. The AFS can prevent the wheel from locking but is worse than the other two methods.

FIGURE 12 Comparison of vehicle response with AFS and DBC under straight-line maneuver on the μ-split road.

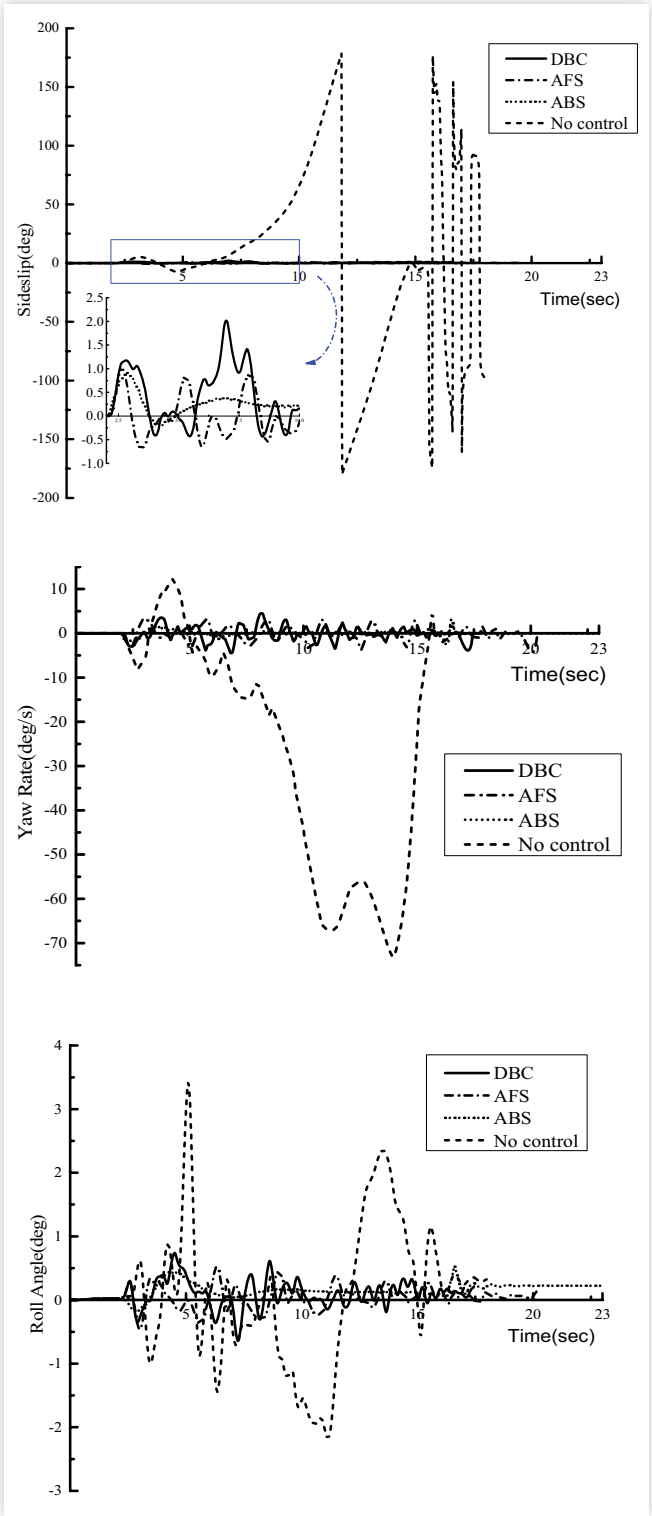

FIGURE 13 Rear outer wheel speed on the μ-split road.

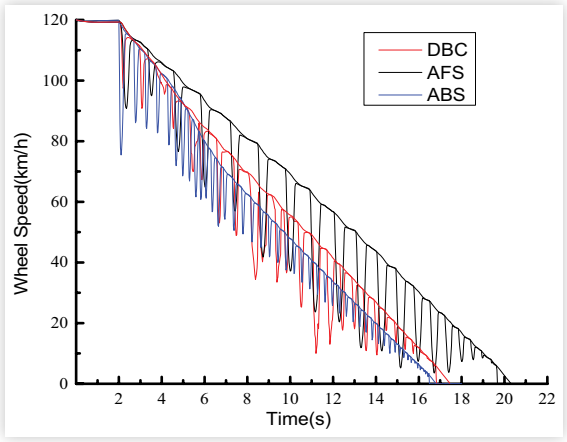

Crosswind Maneuver The vehicle performance is easily affected by the crosswind. Therefore, crosswind condition is selected to verify the resistance of the two proposed strategies. The coach runs straight on the road with adhesion coefficient of 0.2. Air mass density is 1.206 kg/m^3. Crosswind occurs at 2 seconds and the wind ascends to 40 km/h within 1 second. The crosswind heading degree is 90. The coach runs at 100 km/h in the operation. As shown in Figure 14, the simulations show that the coach under no control rotates 360 degrees from the 3rd second to the 15th second. The yaw rate curve with AFS control, without deviating from the desired straight track, shows that AFS method can control the direction of the coach better than DBC. The yaw rate curve with DBC always deviates from zero value, which leads to the deviation from the desired straight track. The results show that DBC cannot change the deflection error of the coach, but it can reduce the sideslip angle and has a better lateral dynamic to withstand the crosswind and effectively reduce the roll angle of the coach.

Rollover Stability Strategy of a Coach

Rollover is that lateral forces cannot provide enough centrifugal force at cornering acceleration, and the vertical forces of one side become zero and detach from the road. By changing the structural parameters of the coach, such as changing the stiffness and damping coefficient of the suspension, the rollover resistance ability of the coach can be enhanced. Adding effectively control strategies can improve the roll stability while driving.

Differential Braking Control Strategy

Differential braking is selected to avoid the rollover of the coach. By applying the independent braking of one side or one wheel, the additional yaw moment of the coach mass

FIGURE 14 Vehicle response of the crosswind in a straight line.

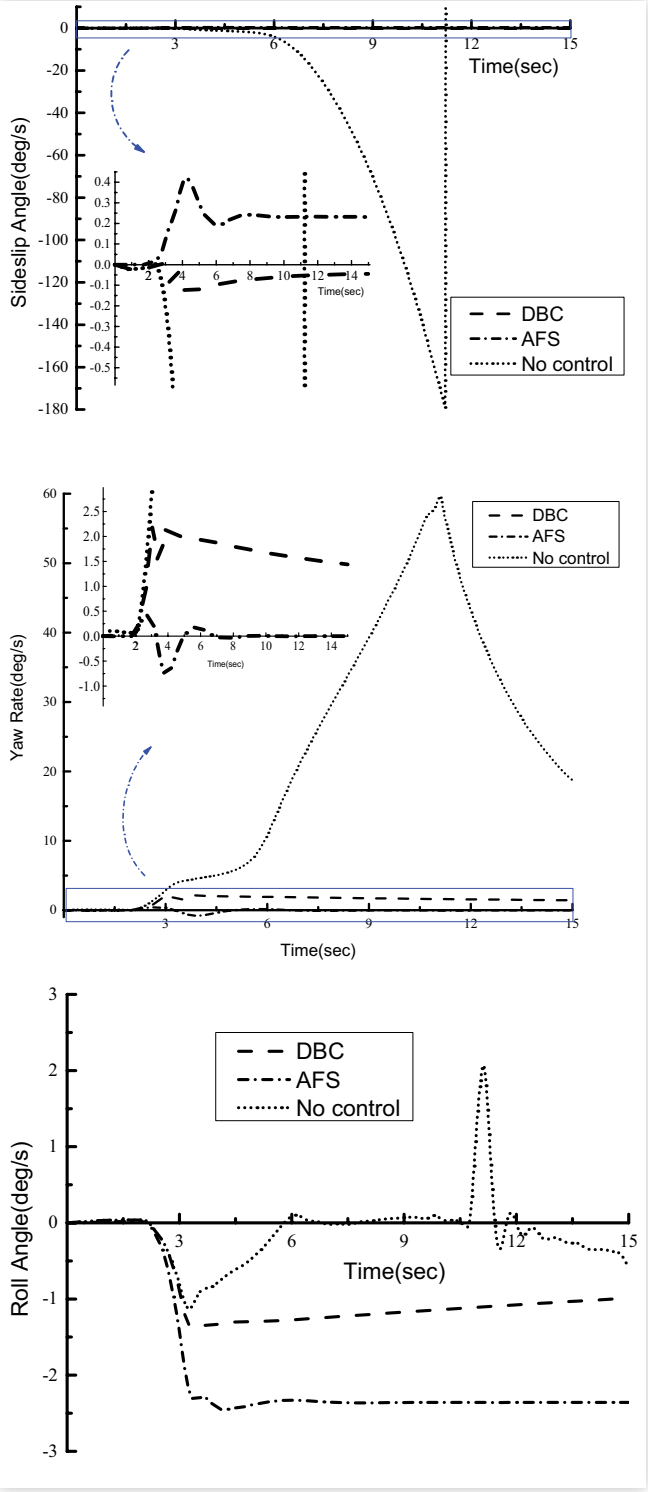

center is changed, which effectively changes the state of the coach and reduces the risk of rollover.

LQR controller is still adopted in the DBC. Rollover prevention control strategy is employed in the RW module to determine whether to actuate the additional yaw moment module. TruckSim transmits the front wheel angle and the longitudinal speed to the 3-DOF vehicle model. The 3-DOF model outputs the reference roll angle and so on. TruckSim outputs actual values. The reference values and actual values are delivered to the RW module. If it is about to roll, it will actuate the additional yaw moment calculation module. And this model calculates the optimal yaw moment the coach needs. Braking force distribution module decides which wheel to brake according to the vertical load of the wheel, and turns additional yaw moment into brake force, and transmits brake force to TruckSim to brake the corresponding wheel.

AFS Control Strategy

Adaptive PID fuzzy controller is still adopted in the AFS and RW module is employed to avoid rollover. TruckSim transmits the front wheel angle and the longitudinal speed to the 3-DOF model. The 3-DOF reference model outputs referenced roll angle and so on. TruckSim outputs actual values. These reference values and actual values are sent to the RW module. If the coach is about to roll, the fuzzy PID self-tuning control module will be triggered. And this model calculates the optimal additional steering wheel angle the coach needs and transmits.

3-DOF Reference Model The body roll angle is required in the roll stability analysis, so the roll movement should be considered on the basis of the yaw movement and the lateral movement, and other movements are ignored. As shown in Figure 15, the 3-DOF coach model only has the rotations

FIGURE 15 Three-DOF model.

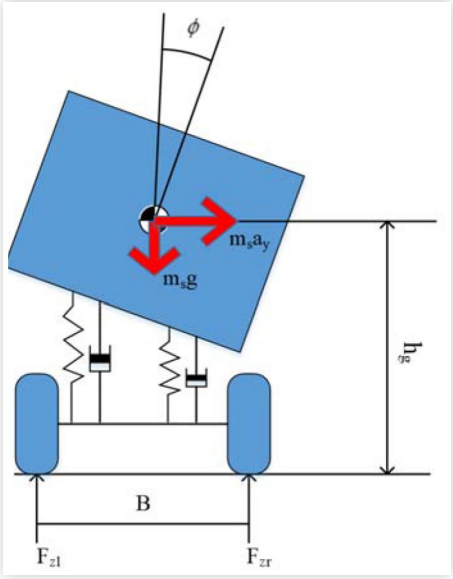

around the *x*- and *z*-axes and the movement along the *y*-axis. Three DOF are characterized by lateral velocity, yaw rate, and roll angle, respectively.

Establish moment equation according to the wheel track center point:

$$m_s a_y h_g + mg\Delta y = \left(F_{zl} - F_{zr}\right)\cdot T/2 \qquad \text{Eq. (32)}$$

where T is the wheel track. As shown in Equation 31, the coach rollover is related to the following factors: the vertical load difference between left and right wheels $F_{zl} - F_{zr}$, the mass of the coach m, the lateral displacement of the mass center related to tread center Δy, coach lateral acceleration a_y, and height of mass center h_g. The motion equations of the coach in three directions are as follows:

Lateral motion:

$$ma_y - m_s h\ddot{\phi} = F_{y_f}\cos\delta + F_{yr} \qquad \text{Eq. (33)}$$

Yaw motion:

$$I_z\dot{\omega}_r = aF_{y_f}\cos\delta - bF_{yr} \qquad \text{Eq. (34)}$$

Roll motion:

$$I_{xeq}\ddot{\phi} - m_s a_y h = m_s g h\phi - C_\phi\dot{\phi} - K_\phi\phi \qquad \text{Eq. (35)}$$

Equations 31-35 are rewritten into state space format as below:

$$\dot{x} = Ax + B\delta_f \qquad \text{Eq. (36)}$$

In the above equation, the state variable is $x = \begin{bmatrix}\beta & \omega_r & \dot{\varphi} & \varphi\end{bmatrix}^T$. The matrices A and B are:

$$A = \begin{bmatrix} \frac{-(k_1+k_2)I_{xeq}}{mI_x v_x} & \frac{(k_1 b - k_2 a)I_{xeq}}{mI_x v_x^2} - 1 & \frac{-h}{I_x v_x} & \frac{h(mgh - K_\phi)}{I_x v_x} \\ \frac{k_2 b - k_1 a}{I_z} & \frac{-(k_1 a^2 + k_2 b^2)}{I_z v_x} & 0 & 0 \\ \frac{-h(k_1+k_2)}{I_x} & \frac{h(k_2 b - k_1 a)}{I_z v_x} & \frac{-C_\phi}{I_x} & \frac{mgh - K_\phi}{I_x} \\ 0 & 0 & 1 & 0 \end{bmatrix}$$

$$B = \begin{bmatrix} \frac{k_1 I_{xeq}}{mI_x v_x} & \frac{k_1 a}{I_z} & \frac{hk_1}{I_x} & 0 \end{bmatrix} \qquad \text{Eq. (37)}$$

where I_{xeq} is the moment of inertia relative to the roll axis. I_{xeq} can be calculated as follows:

$$I_{xeq} = I_x + m_s h^2 \qquad \text{Eq. (38)}$$

Rollover Warning Module Rollover of the coach is indicated by lateral load transfer ratio (*LTR*); in this study *LTR* is defined as the ratio of the difference between vertical load of the left and the right wheels to the total vertical load of the left and right wheels:

$$LTR = \frac{F_{zl} - F_{zr}}{F_{zl} + F_{zr}} \qquad \text{Eq. (39)}$$

Among them, F_{zl} and F_{zr} are vertical loads of the left and right wheels. When $LTR = -1$, F_{zl} is 0, the left wheels have detached from the ground, and the coach slants to the right. When $LTR = 0$, the coach is in a steady state and has no tendency to tilt. When $LTR = 1$, F_{zr} is 0, the right wheels have detached from the ground, and the coach slants to the left. The vertical force of the tires has the following relationship:

$$\begin{aligned} F_{zl}\frac{T}{2} - F_{zr}\frac{T}{2} + C_\phi\dot{\phi} + K_\phi\phi = 0 \\ F_{zl} + F_{zr} = mg \end{aligned} \qquad \text{Eq. (40)}$$

where K_ϕ is the roll stiffness of the coach suspension and C_ϕ is the roll damping coefficient of the coach suspension. In accordance with Equations 40 and 41, LTR can be expressed as:

$$LTR = \frac{2\left(K_\phi\phi + C_\phi\dot{\phi}\right)}{mgT} \qquad \text{Eq. (41)}$$

RW is that the module calculates the current and the future state until the time the coach rollover occurs or the time more than 2 seconds. Set step size $T = 0.05$ s. RW module calculates lateral LTR of the current time and the time after nT. The absolute threshold of *LTR* is set to 0.9. When $LTR > 0.9$, this indicates that the coach is about to rollover. If the calculation is terminated by rollover, RW module will output RW = 1 and actuates the additional torque/angle module. The number of times during the calculation is called rollover time. If the calculation is terminated by overtime, RW module will output RW = 0, and the DBC or AFS do not work. Then enter the next cycle. The purpose of setting the time 2 s is to avoid excessive computation.

The warning process of RW module is shown in Figure 16.

FIGURE 16 Block diagram of RW module.

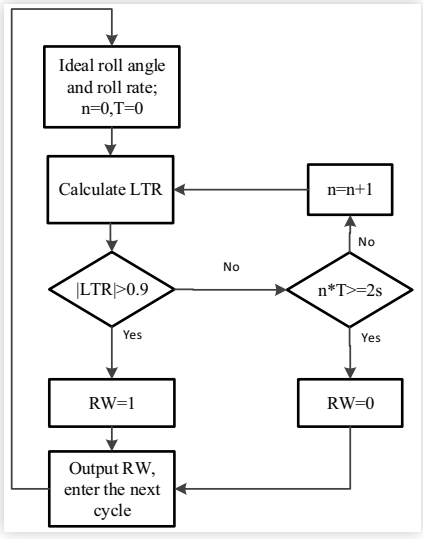

Additional Torque Calculation Module LQR control is used to calculate the optimal additional yaw moment for anti-rollover of the coach. The dynamic state equation of the coach is as follows:

$$\dot{x} = Ax + B\delta + C\Delta M \qquad \text{Eq. (42)}$$

where the state variable x and matrices A and B are the same as the previous 3-DOF reference model. Matrix C is additional yaw moment: $C = \begin{bmatrix} 0 & 1/I_z & 0 & 0 \end{bmatrix}$.

The difference between Equations 36 and 42 is given as below:

$$\Delta\dot{x} = A\Delta x + C\Delta u \qquad \text{Eq. (43)}$$

where Δu in Equation 43 is the additional yaw moment control factor.

The performance index is selected as:

$$J = \frac{1}{2}\int_0^\infty \left(y^T Q y + u^T R u \right) dt \qquad \text{Eq. (44)}$$

The feedback coefficient is $K = \begin{bmatrix} k1 & k2 & k3 & k4 \end{bmatrix}$. The additional yaw moment is:

$$\Delta M_z = -k1\Delta\beta - k2\Delta\omega_r - k3\Delta\varphi - k4\Delta\dot{\varphi} \qquad \text{Eq. (45)}$$

Simulation Results

Sinusoidal Maneuver Sinusoidal maneuver at 70 km/h is conducted to compare the pros and cons of the two control methods. As shown in Figure 17, simulation shows that the DBC and the AFS have similar control effect in sinusoidal maneuver. They can effectively enhance the stability of the coach.

J-Turn Maneuver The operation at 80 km/h is selected to validate the proposed two rollover stability control strategies. The simulation shows that the coach under no control is going to roll at 2.5 s in the operation. Comparing the two strategies, as shown in Figure 18, it can be found that AFS control has a better handling performance than DBC in J-turn maneuver. DBC has a better path tracking ability than the AFS.

Take sinusoidal maneuver as an example to compare the roll and yaw stability control strategy in Figure 19. In the comparison between AFS and DBC, DBC has a better control effect in sinusoidal maneuver. In the comparison between roll and yaw stability control, the roll stability control of AFS control has a smaller sideslip angle and yaw rate than the yaw stability control; the yaw stability control of the DBC has a smaller sideslip angle and roll angle than the roll stability control. In DBC, the yaw control has a faster response. For AFS control, the yaw control reacts faster to sideslip angle and yaw rate, and the roll control reacts faster to roll angle.

FIGURE 17 Vehicle response of 70 km/h sinusoidal maneuver.

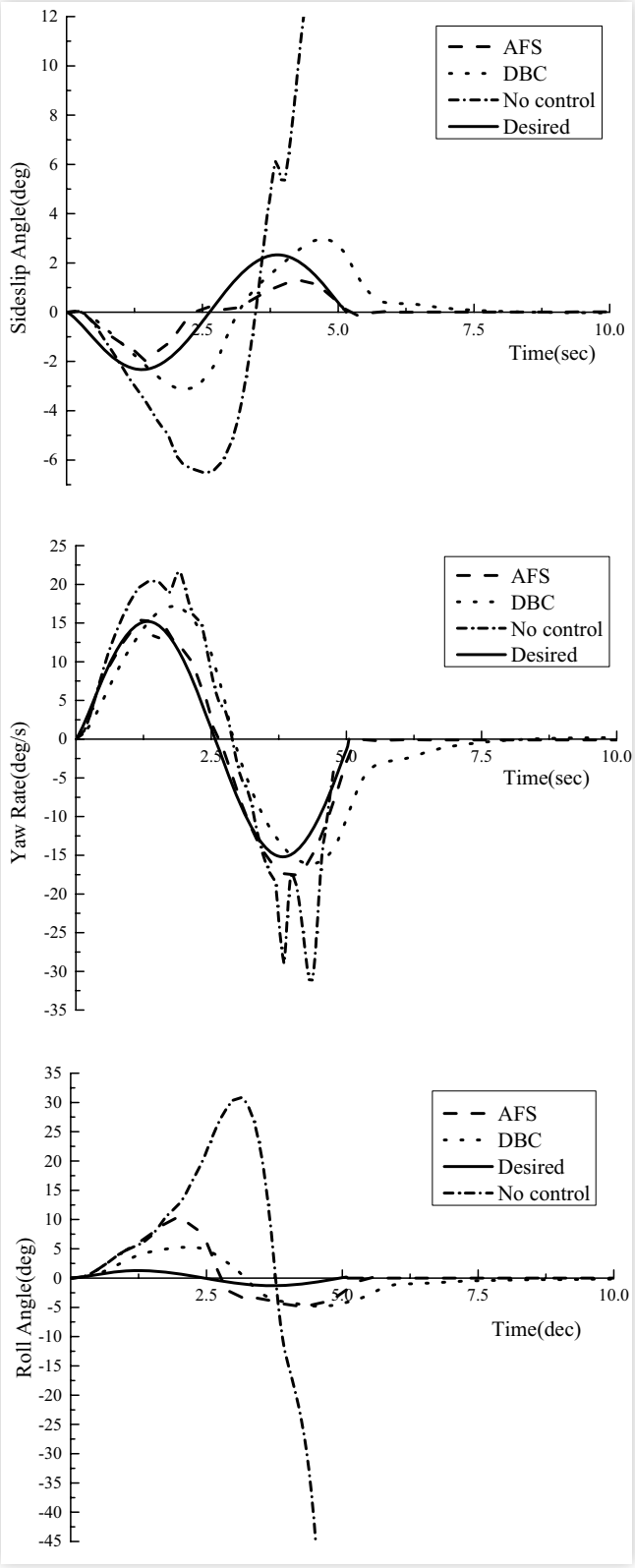

FIGURE 18 Vehicle response of 80 km/h J-turn maneuver.

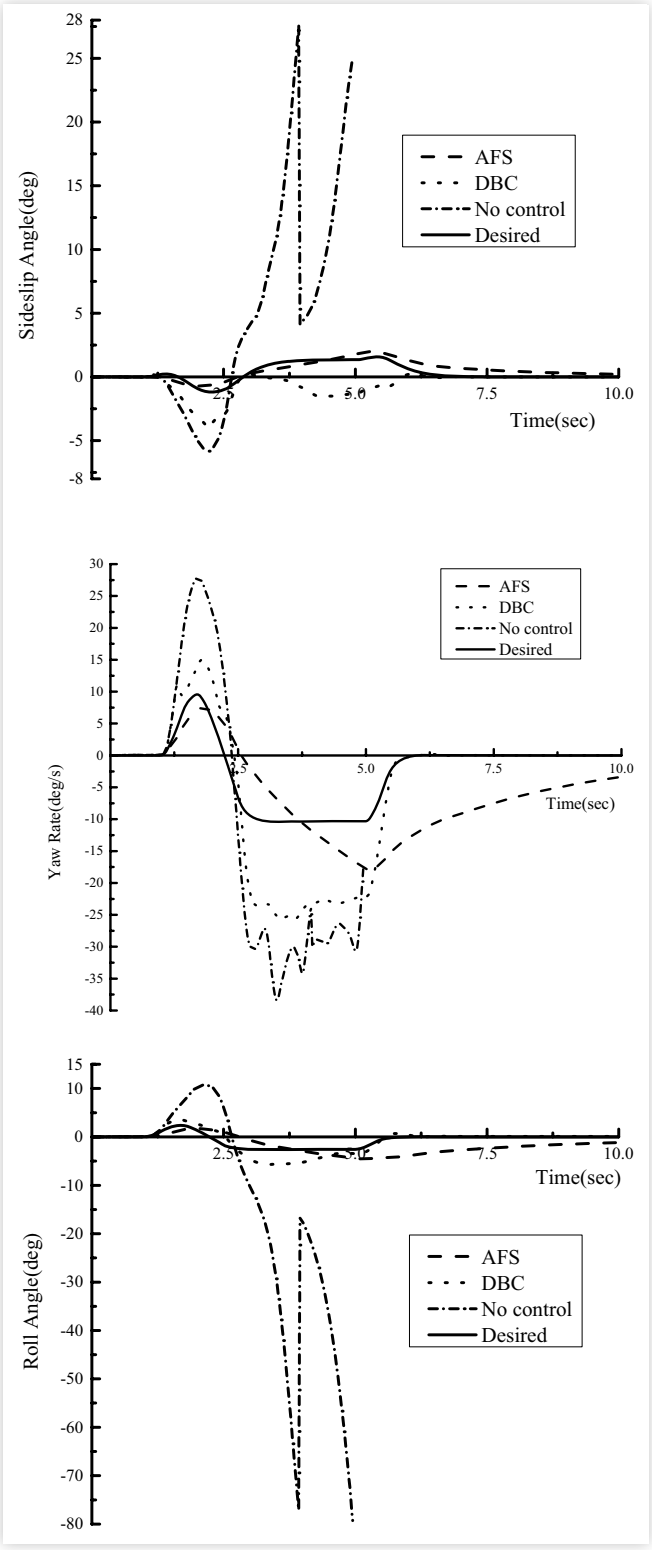

FIGURE 19 Vehicle response of 70 km/h sinusoidal maneuver.

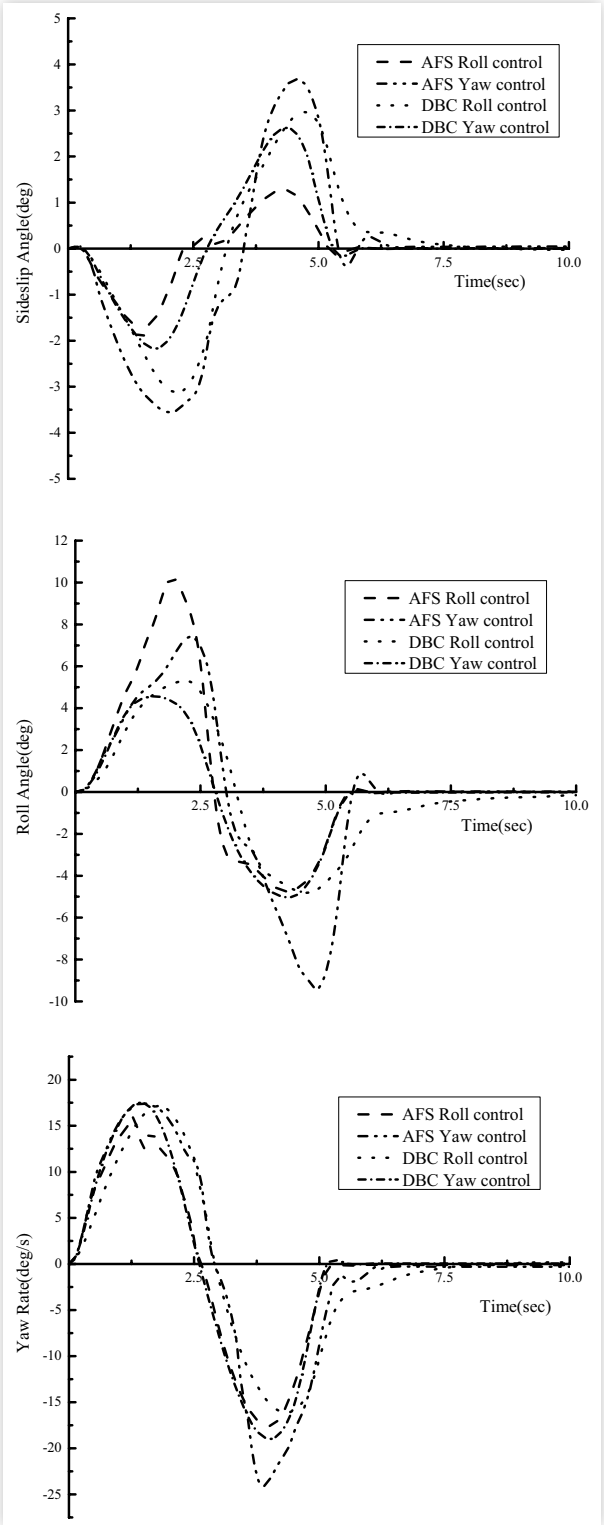

Conclusions

In this article, an AFS control strategy based on a fuzzy PID self-tuning controller and a DBC strategy based on a LQR controller are proposed to improve the coach handling stability and maneuverability. Sinusoidal and J-turn operations are conducted to verify the proposed strategy. The DBC performs better in sinusoidal maneuver and the AFS performs better in J-turn maneuver, but it is not better than the AFS in path tracking capability. Through the establishment of roll control strategies, the results show that the coach handling stability and transient response performance are improved. The two strategies can improve the handling stability of the coach.

Then the two control methods are compared in terms of yaw stability and rollover stability performance of the coach. Sinusoidal, J-turn, straight-line brake on the μ-split road, and crosswind operation maneuvers are simulated to compare the different responses of the two strategies. Both DBC and AFS can prevent yaw and rollover instability through active intervention under various extreme conditions. The DBC method will loss longitudinal speed and cannot provide lane keeping capacity. In contrast, the AFS has a strong lane keeping capacity and no longitudinal vehicle speed loss, but AFS provides limited yaw moment through the change of front wheel angle. However, drivers will prejudge on various working conditions and the route errors will be corrected when driving. Reducing the speed is an important guarantee for the safety of man and vehicles in the extreme conditions. Both methods are important. But DBC is necessary and AFS can provide assistance. In the future, AFS and DBC will be integrated or even more active systems are integrated on coaches and other vehicles. This article compares the effects of DBC and AFS on the yaw/roll stability of a coach under various working conditions and provides reference for future integrated control of coaches. The results show that the AFS and the DBC can enhance the handling stability and effectively prevent rollover of the coach, but each has its own strengths.

Contact Information

Zheng Hongyu
zhy_jlu@163.com
State Key Laboratory of Automotive Simulation and Control
Jilin University Changchun
P.R. China 130025

Acknowledgments

This work was supported by National Natural Science Foundation of China (no. 51575223) and Key scientific and technological project of Science and Technology Department of Jilin Province (20160101275JC and 20170414045GH).

Definitions/Abbreviations

AFS - Active front wheel steering
DBC - Differential braking control
RW - Rollover warning
ABS - Anti-lock brake system

References

1. Van Zanten, A., "Bosch ESP Systems: 5 Years of Experience," SAE Technical Paper 2000-01-1633, 2000, doi:10.4271/2000-01-1633.
2. Her, H., Koh, Y., Joa, E., Yi, K. et al., "An Integrated Control of Differential Braking, Front/Rear Traction, and Active Roll Moment for Limit Handling Performance," *IEEE Transactions on Vehicular Technology* 65(6):4288-4300, doi:10.1109/TVT.2015.2513063.
3. Jonasson, M. and Thor, M., "Steering Redundancy for Self-Driving Vehicles Using Differential Braking," *Vehicle System Dynamics* 55(S1):1-19, 2017, doi:10.1080/00423114.2017. 1356929.
4. Chen, B.C. and Peng, H., "Differential-Braking-Based Rollover Prevention for Sport Utility Vehicles with Human-in-the-Loop Evaluations," *Vehicle System Dynamics* 36(4):359-389, 2001, doi:10.1076/vesd.36.4.359.3546.
5. Esmailzadeh, E., Goodarzi, A., and Vossoughi, G.R., "Optimal Yaw Moment Control Law for Improved Vehicle Handling," *Mechatronics* 13(7):659-675, 2003, doi:10.1016/S0957-4158 (02)00036-3.
6. Fujimoto, H., Tsumasaka, A., and Noguchi, T, "Direct Yaw-Moment Control of Electric Vehicle Based on Cornering Stiffness Estimation," Presented at *the Industrial Electronics Society, 31st Annual Conference of IEEE Industrial Electronics Society, 2005*, USA, Nov. 6-10, 2005.
7. Yi, K., Chung, T., Kim, J., and Yi, S., "An Investigation into Differential Braking Strategies for Vehicle Stability Control," *Proceedings of the Institution of Mechanical Engineers, Part D: Journal of Automobile Engineering* 217(12):1081-1093, 2007, doi:10.1243/09544070JAUTO77.
8. Mizushima, T., Raksincharoensak, P., and Nagai, M., "Direct Yaw-Moment Control Adapted to Driver Behavior Recognition," Presented at *the SICE-ICASE 2006*, Korea, Oct. 18-21, 2006.
9. Zhang, S., Zhang, T., and Zhou, S., "Vehicle Stability Control Strategy Based on Active Torque Distribution and Differential Braking," Presented at *the ICMTMA 2009*, China, Apr. 11-12, 2009.
10. Ghosh, S., Deb, A., Mahala, M., Tanbakuchi, M. et al., "Active Yaw Control of a Vehicle Using a Fuzzy Logic Algorithm," SAE Technical Paper 2012-01-0229, 2012, doi:10.4271/2012-01-0229.
11. Brad, H., Saied, T., Mehdi, A., and Alexander, R., "Yaw Stability Control and Emergency Roll Control for Vehicle Rollover Mitigation," SAE Technical Paper 2010-01-1901, 2010, doi:10.4271/2010-01-1901.

12. Tchamna, R. and Youn, I., "Yaw Rate and Side-Slip Control Considering Vehicle Longitudinal Dynamics," *International Journal of Automotive Technology* 14(1):53-60, 2013, doi:10.1007/s12239-013-0007-1.
13. Elhefnawy, A., Sharaf, A.M., Ragheb, H.M., and Hegazy, S.M., "Active Vehicle Safety Using Integrated Control of Body Roll and Direct Yaw Moment," Presented at *the AMME 2016*, Egypt, April 19-21, 2016.
14. Yu, Z.X., Li, J., Dai, F.G., and Li, S., "Anti-Rollover Control Based on Fuzzy Differential Braking for Heavy Duty Commercial Vehicle," Presented at *the ICMMCT 2016*, China, Jan. 15-16, 2016.
15. Klier, W., Reimann, G., and Reinelt, W., "Concept and Functionality of the Active Front Steering System," SAE Technical Paper 2004-21-0073, 2014, doi:10.4271/2004-01-2081.
16. Oraby, W.A.H., El-Demerdash, S.M., Selim, A.M., Faizz, A. et al., "Improvement of Vehicle Lateral Dynamics by Active Front Steering Control," SAE Technical Paper 2004-01-2081, 2004, doi:10.4271/2004-01-2081.
17. Oraby, W.A., "Improvement of Vehicle Lateral Stability during Overtaking Process by Active Front Steering System," SAE Technical Paper 2007-01-0810, 2007, doi:10.4271/2007-01-0810.
18. Zheng, B. and Anwar, S., "Yaw Stability Control of a Steer-by-Wire Equipped Vehicle via Active Front Wheel Steering," *Mechatronics* 19(6):799-804, 2009, doi:10.1016/j.mechatronics.2009.04.005.
19. Truong, D.T. and Tomaske, W., "Active Front Steering System Using Adaptive Sliding Mode Control," Presented at *the CCDC, 2013*, China, May 25-27, 2013.
20. Elmi, N., Ohadi, A., and Samadi, B., "Active Front-Steering Control of a Sport Utility Vehicle Using a Robust Linear Quadratic Regulator Method, with Emphasis on the Roll Dynamics," *Proceedings of the Institution of Mechanical Engineers, Part D: Journal of Automobile Engineering* 227(12):1636-1649, 2013, doi:10.1177/0954407013502319.
21. Xu, Y.H. and Ahmadian, M., "Study on the Performance of Active Front Steering System," *International Journal of Automotive Technology* 14(4):595-603, 2013, doi:10.1007/s12239-013-0064-5.
22. Kolte, S., Srinivasan, A., and Srikrishna, A., "Development of Decentralized Integrated Chassis Control for Vehicle Stability in Limit Handling," *SAE Int. J. Veh. Dyn., Stab., and NVH* 1(1):1-10, 2017, doi:10.4271/2016-01-8106.
23. Zhang, H. and Wang, J., "Vehicle Lateral Dynamics Control through AFS/DYC and Robust Gain-Scheduling Approach," *IEEE Transactions on Vehicular Technology* 65(1):489-494, 2016, doi:10.1109/TVT.2015.2391184.
24. Zheng, H., Hu, J., and Ma, S., "Research on Simulation and Control of Differential Braking Stability of Tractor Semi-Trailer," SAE Technical Paper 2015-01-2842, 2015, doi:10.4271/2015-01-2842.
25. Elhefnawy, A., sharaf, A., Ragheb, H., and Hegazy, S., "Design of an Integrated Yaw-Roll Moment and Active Front Steering Controller Using Fuzzy Logic Control," *SAE Int. J. Veh. Dyn., Stab., and NVH* 1(2), 2017, doi:10.4271/2017-01-1569.
26. Dornhege, J., Nolden, S., and Mayer, M., "Steering Torque Disturbance Rejection," *SAE Int. J. Veh. Dyn., Stab., and NVH* 1(2), 2017, doi:10.4271/2017-01-1482.
27. Koibuchi, K., Yamamoto, M., Fukada, Y., and Inagaki, S., "Vehicle Stability Control in Limit Cornering by Active Brake," SAE Technical Paper 960487, 1996, doi:104271/960487.

Appendix

TABLE A.1 Main parameters of a coach.

Parameter description	Symbol	Unit	Value
Sprung mass	m_s	kg	6360
Unsprung mass	m_u	kg	1260
Moment of inertia around *X*-axis	I_x	kg·m^2	7695.6
Moment of inertia around *Z*-axis	I_z	kg·m^2	30782.4
Load	m_n	N	3000
Distance between gravity center and front axle	a	m	3.105
Distance between gravity center and rear axle	b	m	4.305
Lateral deflection stiffness of front axle tire	k_1	N/rad	286479
Lateral deflection stiffness of rear axle tire	k_2	N/rad	687549
Roll angle stiffness of vehicle suspension	K_ϕ	N·m/rad	412607
Roll angle damping coefficient of vehicle suspension	C_ϕ	N·m·s/rad	160458
Height of gravity center	h	m	0.69
Wheel track	T	m	2.6